Original Research

Volume 4, Issue 1, pp 30-47, June 2022

ACHIEVERS JOURNAL OF SCIENTIFIC RESEARCH

Open Access Publications of Achievers University, Owo

Available Online at *www.achieversjournalofscience.org*

Litho-Structural Characterization Using Aeromagnetic Data Around Igabi Northwestern Nigeria

Okpoli, C.C.[1*], Oyeshomo, A.V.[1], Akingboye, A.S.[1], Fajana, K.V.[1]

[1]Department of Earth Sciences, Adekunle Ajasin University, Akungba-Akoko Ondo State, Nigeria

E-mail: cyril.okpoli@aaua.edu.ng

Submitted: April 5, 2022 Revised: April 29, 2022 Accepted: May 10, 2022 Published: June 30, 2022

Abstract

The present study aims at delineating basement depth and contact locations, deduced from the available aeromagnetic data around Igabi Northwestern part of Nigeria. Total gradient amplitude and Source Parameter Index techniques were used to calculate the depth to the magnetic basement sources. They reflected similar results for estimating the basement depths ranging from -63051.21*m* to -7639.14 *m*. Furthermore, the tilt angle derivative maps results revealed various anomalous trends and to source depth of magnetic value over 3000 m. Spectral Analyses suggest depth to magnetic sources range from deep, intermediate and shallow with depths between 40 and 60*m* for shallow and 600 *m* to *1200 m* for intermediate and 900 *m* to 3200*m*for deep sources on the magnetic map. The obtained Euler anomalies depths range from <386.5 m to >2054 m for the magnetic map. This study, therefore, suggest rocks that varies in depth based on their lithologies that led to variations in the measured magnetic field parameters in the study area.

Keywords: Aeromagnetic; Derivatives; Spectral Analyses; Igabi; Northwestern Nigeria

1.0 Introduction

The magnetic method is extensively used for determining the depth to magnetic crystalline rocks and especially the basement underlying surface sediments and sedimentary rocks, which are essentially transparent to magnetic fields (Hinze *et al.,* 2013). A large proportion of older basement regions of Igabi is covered with a variable thickness of sedimentary materials, which obscures most direct geological signatures of, the basement architecture. Interpretations of magnetic survey data provide a means to gaining an indirect insight into the underlying geology and to the magnetic source (Milligan *et al.,* 2004).

Mineral exploration activity continues to spread from areas of outcropping and sub-cropping basement into areas with greater thickness of cover. For resource exploration purposes, one of the most useful inferences that may be derived from analyses of magnetic field data is the depth of crystalline basement beneath the cover (Milligan *et al.,* 2004). The depth and the edges of causative bodies are important parameters, providing information that becomes a guide for the subsequent exploration processes, such as

drilling and ore body modeling. The total field magnetic data is usually the first data set to be collected in geophysical exploration (Ghosh *et al.,* 2012). With the large quantities of data now available for investigation in the country, it is desirable to use computerized methods of estimating depth to basement. A number of such methods have been published over the last few decades, with one of the most enduring being Euler deconvolution (Thompson, 1982). This has recently undergone reappearance in popularity, with extensions to the original method now providing a solution of structural indices as well as other parameters (Reid *et al*., 1990; Nabighian and Hansen, 2001; FitzGerald *et al.,* 2003).

Cordell and Grauch (1985) developed the horizontal derivative method to locate the horizontal position of the density or magnetization boundaries. Hansen *et al*. (1987) used the horizontal gradient magnitude and the analytic signal for interpreting edges and dips in magnetic anomaly data. Li (2003) has published a useful summary and guidelines for best use of several depth estimation methods, including Euler and radial average spectrum. A large number of research papers have been published over the last decade on this subject (e.g., Tsepav, 2018; Gallardo-Delgado *et al.,* 2003; Martins *et al.,* 2010; Martins *et al.,* 2011a; Martins *et al.,* 2011b; Silva *et al.,* 2006; Silva *et al.,* 2007; Silva *et al.,* 2010a, Silva *et al.,* 2010b; Barbosa *et al.,* 1997, Barbosa *et al.,* 1999a; Barbosa *et al.,* 1999b). The tilt angle derivative or has been used as the basis for a variety of methods for edge enhancement of magnetic field anomalies, such as (Cooper and Cowan, 2006; Cooper, 2013; Ferreira *et al.,* 2013). Verduzco *et al*. (2004) enhanced this method so that it could be applied to grid data and suggested using the total horizontal derivative of the tilt angle as an edge detector. Salem *et al.* (2007) exhibited a contact-depth estimation approach based on the tilt angle derivative or tilt horizontal derivative of the magnetic data which was called the tilt-depth method.

Okpoli and Akingboye (2020) studied Igabi area using aerogravity technique to delineate the subsurface crustal architectures and the possibility of hosting mineralized ores. Their studies discovered mineralized ores (Uranium and Amethyst) and estimated depths of the various minerals and how it can be harnessed for economic development of Nigeria. Okpoli *et al.* (2022) investigated Iwo-Apomu region of southwestern Nigeria using integrated remote sensing and aeromagnetic methods in delineating the mineral potential of the of the study area and their approach was able to characterized the several minerals ores in the study area. The validation of both methods suggested clear evidence of the abundance of mineralized ores and possible ways it could be harnessed and used for the national development None of the previous studies utilized source parameter imaging (SPI), spectral analyses (in four quadrants) Euler deconvolution using two source indices for depth estimation of mineralized ores.

In this paper, an approach for the source depth determination (Quantitative interpretation) with reference to the total field magnetic map using Euler deconvolution, Tilt horizontal or tilt angle derivative, Source parameters imaging and average power spectrum results of the 2D airborne magnetic data around Igabi is presented.

2.0 Geologic Setting of the Area

The area lies between longitude 7^0 30' and 8°E and latitude 10^0 30' and 11° N within the Basement Complex of North-Central Nigeria. The study area lies about 30 kilometers southwest of Zaria, approximately an area of 253.57 km^2. The rocks of the area are mostly Precambrian in age and are of the Pan African Orogeny. This thermo tectonic event has virtually obliterated the imprints of earlier events but left its own structural earmarks, which include: faulting, fracturing, shearing, granitic emplacement and granitization (Oyawoye, 1964; Rahaman and Ocan, 1987; Mccurry, 1975; Hubbard, 1975). These areas are considered to be Upper Proterozoic Supracrustal rocks which have been in folded into the Migmatite-Gneiss-Quartzite complex. The lithological variations of the area include fine to coarse grained clastics, pelitic Schists, phyllites, carbonate rocks (marbles/dolomitic marbles) and

mafic metavolcanics (Amphibolites) (Obaje, 2009).

The Migmatitic-Gneiss Complex which underlies most of the Kaduna-Zaria area and the area of investigation is characterized by spectacular exposure of well-defined Migmatite around Kadenda, Kakau, Jagi, Baushe, Sabon Tasha, Kabala east and west areas in Kaduna metropolis. These materials are usually liable to form aquitard and permeable zones to the bedrocks in the country rocks area. (Ogezi, 1988).The lineament/faults associated with these basement complex rocks usually show NE-SW and NW-SE trends (Figure 2).

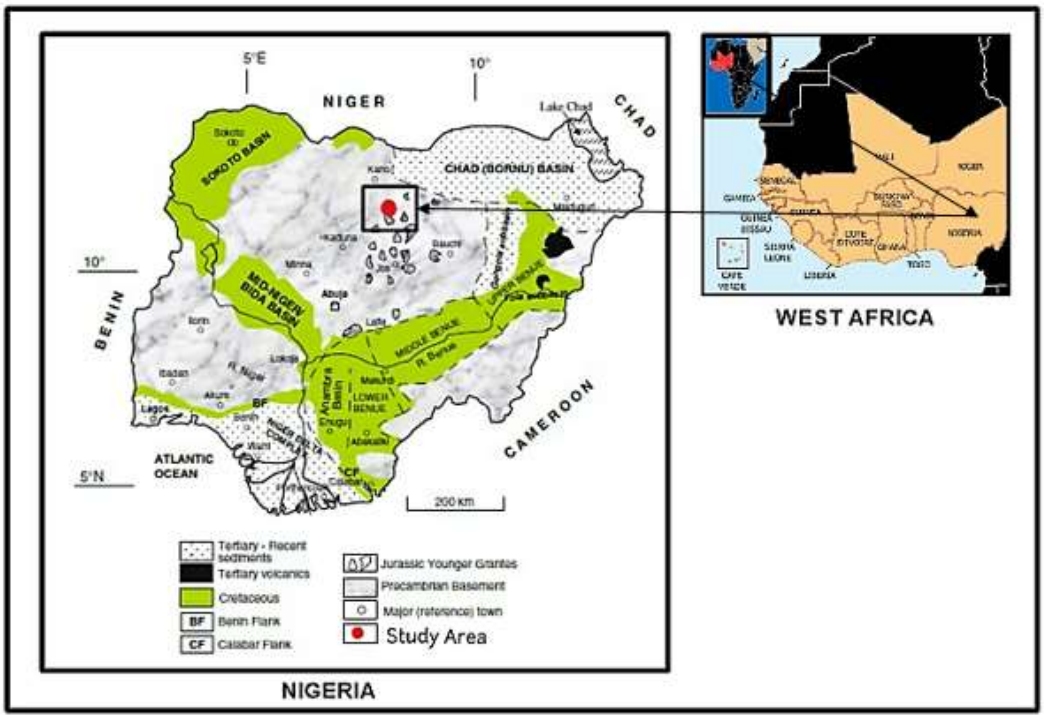

Figure 1: Geological Map of Nigeria showing the study area (Modified after Obaje, 2009).

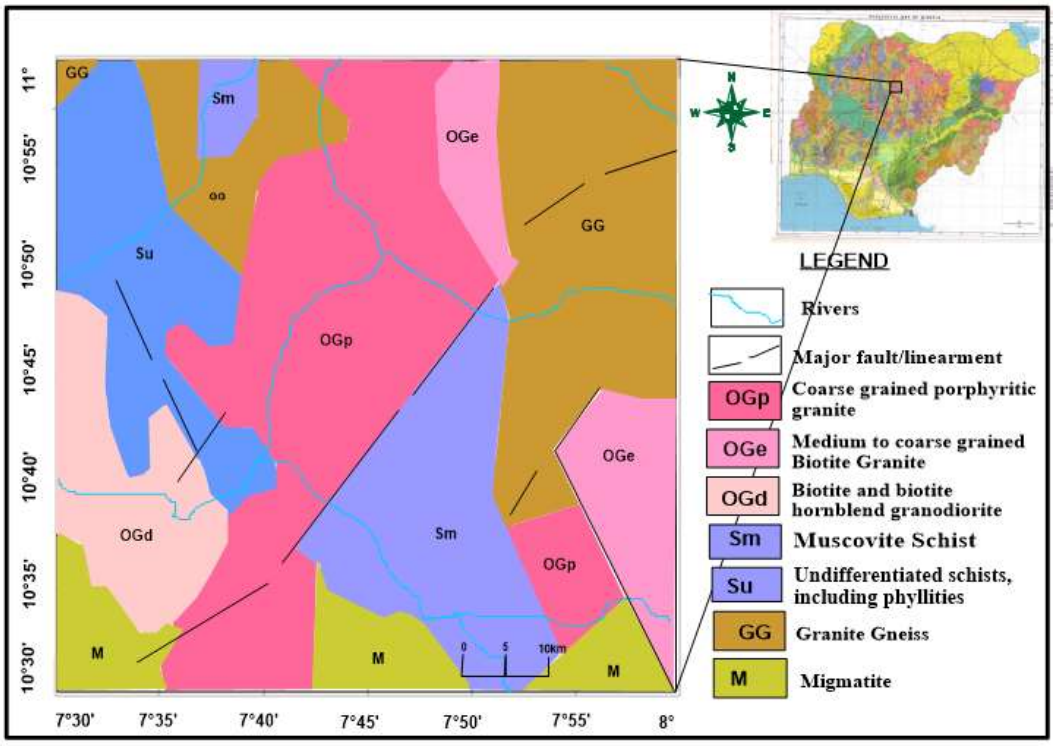

Figure 2: Geological Map of the Study Area (Modified after NGSA, 2010)

3.0 Materials and Method

3.1 Materials Used for the Study

The data sets used for this research and the software package are:

- Grid and line Aeromagnetic data covering Igabi Area Sheet 124 (1: 404922).
- Geosoft
- +® Oasis Montaj™ software version 6.4.2 H.J.
- A digitized map of the Study Area

3.2 Methods

The data was processed using Geosoft® Oasis Montaj™ software, other software include; Surfer and Microsoft Excel.

Data reductions such as: removal of near surface noise (NSN), tilt-angle derivative (TDR) or total horizontal derivative (THDR_TDR)**,** radial average power spectrum (RAPS)/spectral plot and Euler deconvolution were performed for better result output.

The data reductions and enhancements were done using the MAGMAP Step-by-Step filtering processing. The Magnetic data processing flow chat in Figure 3 shows the data processing stages employed.

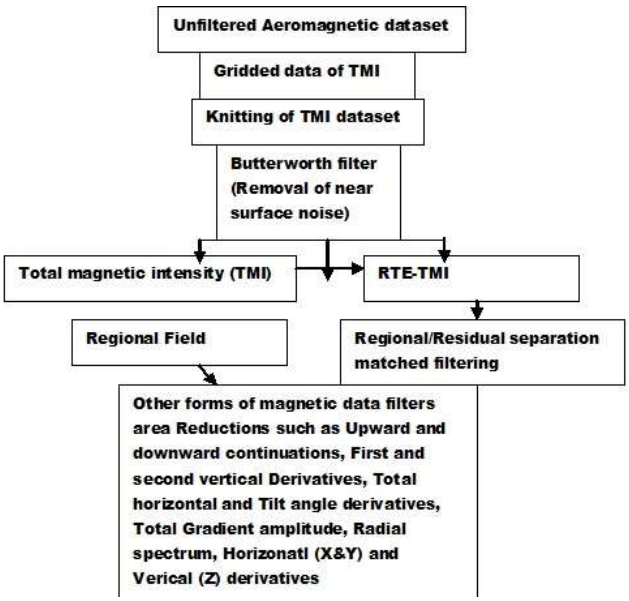

Figure 3: Data Processing and interpretation Flow Chat.

3.2.1 Re-projection of Coordinates and Near Surface Noises (NSN) Removal

The NGSA Total Magnetic Intensity (TMI) data coordinates were re-projected from UTM Zone 32N to UTM Zone 31N of the Greenwich Mercator. This was necessary because the coordinates of the data must correspond to their actual locations. These re-projected data were gridded and adopted as the new TMI data and was filtered to remove Near Surface Noises (NSN) caused by metallic materials, fences, cables (both buried and surface), flight height, etc.

3.2.2 Total Gradient Amplitude

The Total Gradient Amplitude method (Nabighian, 1972; Roest *et al*., 1992) assumes that the sources are isolated dipping contacts separating thick geologic units. Peaks in the Total Gradient Amplitude, which is derived from the first horizontal and vertical derivatives of the observed magnetic field, are used to locate the contacts and estimate their strike directions. If the geologic units are not thick, the depth estimates from the analytic signal method will be too shallow. The dip of the contact can be estimated if the magnetization vectors are assumed to be collinear with the geomagnetic field vector. The Total Gradient Amplitude method is moderately sensitive to noise in the data and interference effects between nearby sources. This transformation is often useful at low magnetic latitudes (e.g. the study area), because of the inherent problems with the RTE, (at such low latitudes). The Total Gradient Amplitude (TGA) is the square root of the sum of the squares of the derivatives in the x, y and z directions (Al-Badani *et al.*, 2017). The expression below illustrates the analytic signal equation:

$$AS = \sqrt{\left(\frac{\partial f}{\partial x}\right)^2 + \left(\frac{\partial f}{\partial y}\right)^2 + \left(\frac{\partial f}{\partial z}\right)^2} \qquad (1)$$

Where, $\frac{df}{dx}\frac{df}{dy}\frac{df}{dz}$ are the first derivatives of the total magnetic field (FVD). It is very useful in locating the edges of magnetic source bodies. The advantage of using AS technique to determine magnetic parameters from magnetic anomalies is the independence of magnetization direction (inclination).

3.2.3 The Tilt-angle Derivative (TDR) and Total Horizontal Derivative (THDR_TDR)

TDR and THDR_TDR are used for mapping shallow basement structures and mineral exploration targets. TDR is used for enhancing

features and causative body edge detection in potential field images (Miller *et al.*, 1994). This filter is defined as:

$$TDR = \tan^{-1}\frac{\mathrm{VDR}}{\mathrm{THDR}} \qquad (2)$$

The Tilt derivative (TDR) is similar to the local phase, but uses the absolute value of the horizontal derivative in the denominator. Due to the nature of the arctan trigonometric function, all amplitudes are restricted to values between $+\pi/2$ and $-\pi/2$ (+90°and -90°) regardless of the amplitudes of Vertical Derivative (VDR) or Total Horizontal Derivative(THDR) (Salem *et al.*, 2008). The Tilt derivatives vary markedly with inclination but for inclinations of 0^o and 90^o, its zero crossing is located close to the edges of the model structures. Positive values are located directly above the sources while negative values are located away from them. Furthermore, the horizontal distance from the 45^o to the 0^o position of the tilt angle is equal to the depth to the top of the contact or the half distances between – 45 m and +45 m (Salem *et al.*, 2008; Okpoli and Eyitoyo, 2016). The total horizontal derivative of the TDR is independent of inclination, similar to the Analytic signal, but is sharper, generating better defined maxima centered over the body edges, which persist to narrower features before coalescing into a single peak.

THDR_TDR is the square root of the sum of the squares derivatives of the tilt angle in the x and y directions.

$$\text{THDR-TDR} = \sqrt{\left(\frac{\partial \mathrm{TDR}^2}{\partial \mathrm{X}}\right)} + = \sqrt{\left(\frac{\partial \mathrm{TDR}^2}{\partial \mathrm{Y}}\right)} \qquad (3)$$

3.2.4 Source Parameter Imaging Method

The Source Parameter Imaging (SPI) method is a technique that uses an extension of the complex analytic signal to estimate magnetic depths. It is profile or grid-based and the solutions show the edge locations, depths, dips and susceptibility contrasts. The method utilizes the relationship between source depth and the local wavenumber (*k*) of the observed field, which can be calculated for any point within a grid of data through horizontal and vertical gradients (Thurston *et al.*, 1997) with the depth usually displayed as an image. The complex analytic signal A1(*x,z*) as defined by (Nabighian, 1972) is expressed as:

$$\mathrm{A}_1(\mathrm{x},\mathrm{z}) = \frac{\partial \mathrm{M(x.z)}}{\partial \mathrm{x}} - j\frac{\partial \mathrm{M(x,z)}}{\partial \mathrm{z}} \qquad (4)$$

where M(*x,z*) is the magnitude of the anomalous total magnetic field,*j* is the imaginary number, and *z* and *x* are Cartesian coordinates for the vertical direction and the horizontal direction perpendicular to strike, respectively. (Nabighian, 1972) showed that the horizontal and vertical derivatives comprising the real and imaginary parts of the 2D analytic signal are related by:

$$\frac{\partial \mathrm{M(x.z)}}{\partial \mathrm{x}} \Leftrightarrow -j\frac{\partial \mathrm{M(x,z)}}{\partial \mathrm{z}} \qquad (5)$$

where ⇔ signifies a Hilberts transform pair. The local wavenumber, *k*1, is defined by (Thurston et al 1997) as:

$$\mathrm{k}_1 = \frac{\partial}{\partial \mathrm{x}}\tan -1\ \left(\frac{\partial \mathrm{M}}{\partial \mathrm{z}} / \frac{\partial \mathrm{M}}{\partial \mathrm{x}}\right) \qquad (6)$$

The analytic signal uses the Hilbert transform pair such that the Hilbert transform and the vertical derivative operators are linear. Therefore, the vertical derivative of equation (2) yields:

$$\frac{\partial^2 \mathrm{M(x.z)}}{\partial \mathrm{z}\,\partial \mathrm{x}} \Leftrightarrow -j\frac{\partial^2 \mathrm{M(x,z)}}{\partial \mathrm{z}^2} \qquad (7)$$

This can be used in defining the analytic signal based on second order derivatives

$$\mathrm{A}_2(\mathrm{x},\mathrm{z}) = \frac{\partial^2 \mathrm{M(x.z)}}{\partial \mathrm{z}\,\partial \mathrm{x}} \Leftrightarrow -j\frac{\partial^2 \mathrm{M(x,z)}}{\partial \mathrm{z}^2} \qquad (8)$$

which yields a second order local wave number $\mathrm{k}_2$given by

$$\mathrm{k}_2 = \frac{\partial}{\partial \mathrm{x}}\tan -1\ \left(\frac{\partial^2 \mathrm{M}}{\partial \mathrm{z}^2} / \frac{\partial^2 \mathrm{M}}{\partial \mathrm{z}\,\partial \mathrm{x}}\right) \qquad (9)$$

The first and second – order local wavenumbers are used to determine the most appropriate model and depth estimate independent of any assumption about a model.
(Nabighian, 1972) derived the expressions for the first and second order local wave numbers as:

$$\mathrm{k}_1 = \frac{(\mathrm{n_k}+1)\mathrm{h_k}}{\mathrm{h}^2\mathrm{k}+\mathrm{x}^2} \qquad (10)$$

and

$$k_2 = \frac{(n_k+2)h_k}{h^2k + x^2} \qquad (11)$$

where $n_k$is the SPI structural index (subscript k = c, t or h), and n_c=1 and n_h = 2 for the contact, thin sheet and horizontal cylinder models and h_k is the depth to the top of the contact, respectively.

For the dipping contact, the maxima of k are located directly over the isolated contact edges and are independent of the magnetic inclination, declination, dip, strike and any remnant magnetization. The depth is estimated at the source edge from the reciprocal of the local wavenumber, as follows (Thurston, 1997):

$$\text{Depth}_{(x=0)} = \frac{1}{K_{max}} \qquad (12)$$

where K_{max} is the peak value of the local of number K over the step source.

3.2.5 Average Power Spectrum

Each wavelength's power unit can be plotted against wavenumber regardless of direction, to produce a power spectrum. In frequency domain, one can prepare and analyze the distribution of short to long wavelength across all measured high to low frequency. The power spectrum can be broken into series of straight lines segments and each segment represents the cumulative response of a discrete assemblage of sources at a given depth. The depth is directly proportional to the slope of the line segment (Spector and Grant, 1970). Potential field may be considered as representing a series of interfering waves of different wavelengths and directions.

The slope of each segment provides information about the depth to the bottom of the magnetic bodies (Kivior and Boyd, 1998). Radially averaged power spectrum of magnetic data according to Blanco-Montenego *et al*. (2003) is expressed as a function of wavenumber and is related to depth to the bottom of the deepest sources as expressed below:

$$K_{max} = \frac{\log zb - \log zt}{zb - zt} \qquad (12)$$

Where Z_t and Z_b are depth to top and bottom of the magnetic sources respectively. K is a function of wavenumber which is expressed in radian per unit distance.

In this study, power spectrum analysis was carried out on aeromagnetic data using Geosoft® Oasis Montaj™ software to identify average depths of source assemblage. This same technique was also adopted to attempt identification of the characteristic depth of the magnetic basement, on a moving window basis, merely by selecting the steepest and therefore straight line segment of the power spectrum, assuming that this part of the spectrum is sourced consistently by basement surface magnetic.

3.2.6 Euler Deconvolution

Euler Deconvolution (ED)is a well-known method to determine the shape of causative bodies from potential field data. Hood, 1965 uses this method for aeromagnetic data interpretation and demonstrated that, the method is valid for point–pole and point–dipole sources. Thomson (1982) elaborates the application of the method to 2D sources and derived the structural indices for several elementary bodies. Reid *et al.* (1990) extended the method to three dimensions and discusses its applicability to gravity anomalies of finite steps and magnetic anomalies of thin dikes and sloping contacts. The use of Euler deconvolution has emerged as a powerful tool for the direct determination of depth and probable source geometry in the magnetic data interpretations. The method can locate or outline the confined sources, dykes and contacts with remarkable accuracy. The Euler deconvolution has been widely used in the automatic interpretation, because it requires no prior knowledge of the source direction and assumes no particular interpretation model. Usually the structural index (SI) is fixed and the locations and depths (x_0, y_0, z_0) of any sources are found using the following equation:

$$\frac{\partial f}{dx}(x - x_o) + \frac{\partial f}{dy}(x - y_o) + \frac{\partial f}{dz}(x - z_o) = SI\,(B - f) \qquad (13)$$

Where f is the observed field at location (x, y, and z) and B is the base level of the field regional value at the points x, y, z and SI is the structural index

or degree of homogeneity (Reid *et al.,* 1990). Equation (13) is solved for the source position by least-squares inversion of a moving window of data points. To obtain an accurate estimate of the source location, the field data used must adequately sample the anomalies present in the data. Accordingly, ED requires four sets of grids as input data; the total magnetic field, first horizontal derivative in x, y and vertical derivative in z-direction. It is insensitive to magnetic inclination and declination. Therefore, the north–south extending geologic features reflect a low signal to noise ratio in the data and therefore, reduction to the pole (RTE) data can be applied to improve this situation (Durrheim *et al.,* 1998). The size of window should be chosen large enough to incorporate substantial variation of the field gradients and it should be small enough not to include significant effects from multiple sources i.e. The board anomalies arising from deep sources are poorly represented in small windows and vice versa. The quality of depth estimation depends on the choice of the correct structural index and adequate sampling of data. Therefore, the choice of the SI and electing of optimum criteria for selecting solutions are fundamental requirements for successful application of this method (Al-Badani *et al.,* 2017).

4.0 Discussion of Results

4.1 Total Magnetic Intensity (TMI) Map

The re-projected data were gridded and adopted as the new Total Magnetic Intensity **(**TMI) data and were filtered to remove Near Surface Noises (NSN) caused by metallic materials, fences, cables (both buried and surface), flight height, etc. Figure 4 demonstrate the analyzed results of the TMI ranging from -30.43 to 51.81 denoting variations in magnetic properties of the subsurface rocks. The TMI map (Figure 4) show positive magnetic intensity value as high as 51.18 nT which dominated almost half of the entire area, covering the central to the northern and very small segment of the southwestern part of the study area. The larger part of the northeastern part of the data marked as Q is characterized with a very high magnetic intensity (51.81 nT). The presence of deeper and rich in mafic minerals rocks in the area may account for the very high magnetic intensity. Long narrow lineaments/faults are clearly seen on the TMI map trending mostly in the NW-SE and NW-SW directions. While the southwestern, southeastern and southern portion of the area (G, C, and E) reveal relatively low to moderate magnetic intensity values (4 - 30.93 nT), this may possibly be attributed to varying degree of deformation. The area of lowest magnetic intensity (-8.69 nT to -90.93) is more prominent in the southeastern part of the area. These variations are results of different mineral compositions, tectonic framework and structural features that are the major contributors to difference in magnetic intensities observed in the entire area. There are narrow lineaments/faults trends marked with point F has the magnetic intensity (-30.93 nT) seen in the north-western part of the area. The trends of these lineaments/faults coincide with the most lineaments/faults trends of the study area as seen in Figure 1.

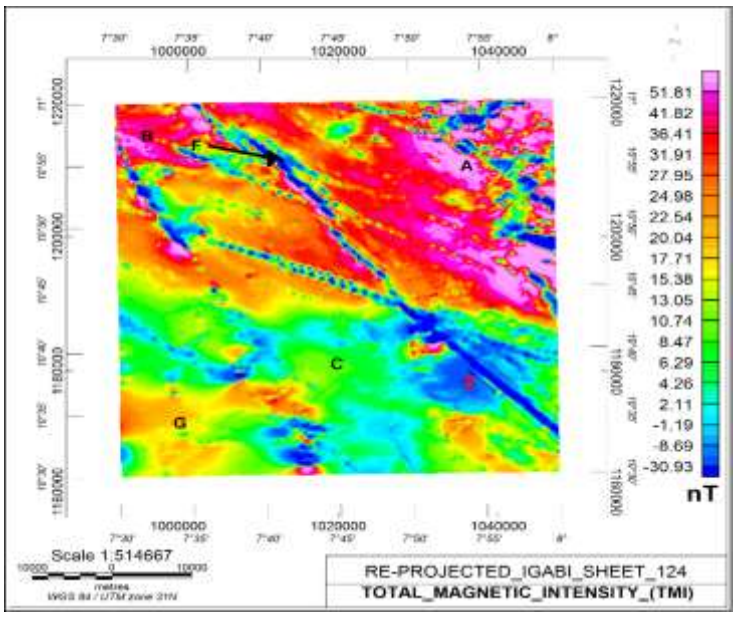

Figure 4: The Total Magnetic Intensity (TMI) map

**Point A indicate area of very high magnetic intensity. Points G, C, E reveals relatively low to moderate magnetic anomaly. Point F show the lineament/faults line and their trends*

4.2 Total Gradient Amplitude

The Total Gradient Amplitude filter produces a particular type of calculated magnetic anomaly enhanced map used in defining edges (boundaries) of geological anomalous magnetization distribution present in maps. It can also be used to determine depth of the anomaly sources. The filter's ability to generate a maximum value directly over the causative body and depth estimation make it a highly useful technique for potential data interpretation (Ansari and Alamdar, 2009). The advantage of this potential field data enhancement method is that its amplitude function is always positive and does not need any assumption of the direction of body magnetization (Jeng *et al.*, 2003).

Figure 5 highlights variations in the magnetization of the magnetic sources in the study area and accentuates the discontinuities and anomaly textures. Figure 5 displays magnetic zone with high analytic signal with respect to depth of 3051 m on the map and occurs in a disperse form in the northwestern and northern parts of the map. The low total gradient amplitude (Blue colour) show the deeper source value of -6773.64 m. The lineaments/faults are trending in NW-SE direction. The area with low total gradient amplitude (blue colour) tends to be deeper in depth than the area of high total gradient amplitude. The total gradient amplitude revealed low to high amplitudes which suggested migmatites, schistose, porphyritic granites, acidic rocks, fractures and biotite granites, gneissic and basic rocks respectively

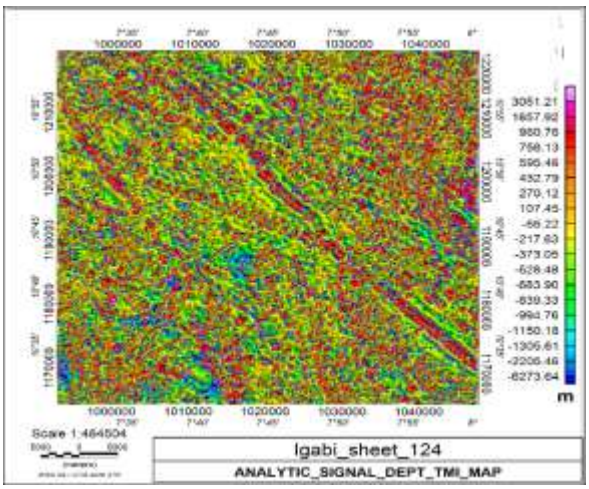

Figures 5: TMI Total Gradient Amplitude Map

4.3 Total Horizontal Derivative-Tilt Derivative (THDR_TDR)

The Total Horizontal Derivative-Tilt Derivative THDR_TDR preserves the amplitude enhancement by its ability to define edges of well-defined maxima. So, the amplitude of the THDR_TDR is related to the reciprocal of the depth to the top of the source (Rajaram, 2009). The THDR_TDR map results helps predict the horizontal location and extent edge of anomaly sources by assuming a vertical contact modeled (Saad, 2017). The Tilt horizontal derivative maps in Figure 6 have magnetic intensity that ranged between 0.0005 and 0.0075 1/m. From the map, one can interpret different geological structures present on the map (Figure 6). The high magnetic intensity with respect to depth (0.0050 – 0.0053 1/m) show most of the lineaments/faults present in the area with their trends. The very low magnetic intensities (0.0005-0.0008 1/m) tends to be deeper (2000 *m)* when compared to other magnetic anomaly present on the map. This deformation was as a result of the pronounced metamorphism and remobilization.

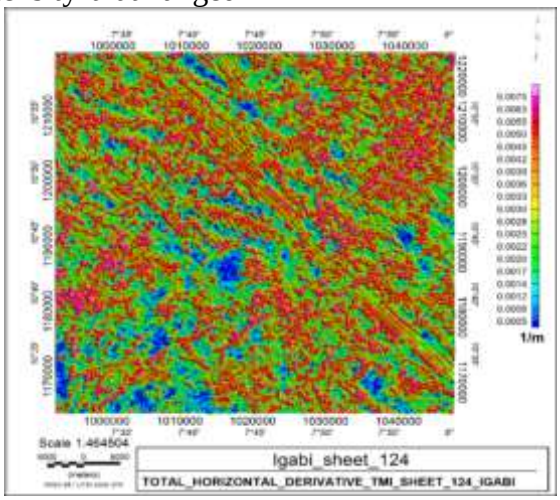

Figure 6: Color shaded total horizontal derivative magnetic map

4.4 Source Parameter Imaging (SPI)

Figure 7 illustrate the result of SPI image, where correct depth estimate for each anomaly can be determined. The results of the depth estimates from application of Source Parameter Imaging method in the study area revealed depth solutions ranging from about -6452.00 m to 2056.67 m for the magnetic map (Figure 7). The SPI-TMI depth map (Figure 7) shows a good similarity to the depth map constructed by using total gradient amplitude technique. On the SPI depth grid shown in Figure 7, the pink areas indicate the shallowest portions of the study area while the blue portions highlight the deepest pockets for both maps.

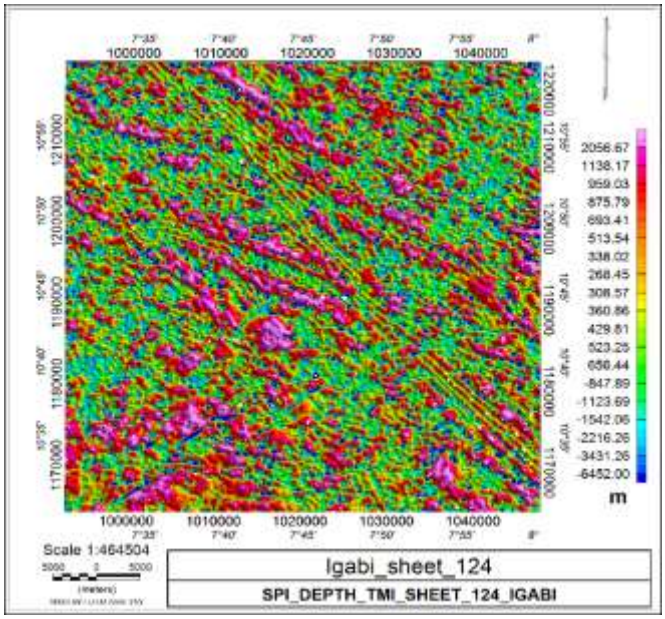

Figure 7: Source Parameter Index (SPI) TMI Map

4.5 Radial Average Power Spectrum (RAPS)

Power Spectrum is a 2D function of the energy and wave number and can be used to identify average depth of source assemblages (Spector and Grant, 1970). The application of power spectrum is a well-established tool for estimating the depths of magnetized bodies (Emberga and Timothy, 2014; Bhattacharyya, 1966; Mishra and Naidu, 1974; Blakely, 1996). Several authors, such as Spector and Grant (1970); Garcia and Ness (1994); Tatiana and Angelo (1998), Okpoli and Akingboye, (2019, 2020) explained the spectral analysis technique. The RAPS TMI was divided into four major quadrants (Figures 8a, b, c and d) to locate the average of source present in the area. The result also shows three layers that are based on the wavelength of the magnetic sources. The deeper source (red line), the intermediate source (yellow line) and the shallower source (blue line). The directions and various depths are illustrated in table 1.

Table 1: Depth estimates from magnetic spectral analysis

Spectral Block	Easting		Northing		Depth of source rocks (m)		
	X_{min}	X_{max}	Y_{min}	Y_{min}	Shallow	Intermediate	Deep
1	994826	1020228	1193663	1221720	40	600	900
2	1019882	1050826	1192046	1221605	90	1960	3300
3	992743	1018007	1164492	1191787	54	2200	3800
4	1018571	1047443	1164831	1190771	60	1200	3200

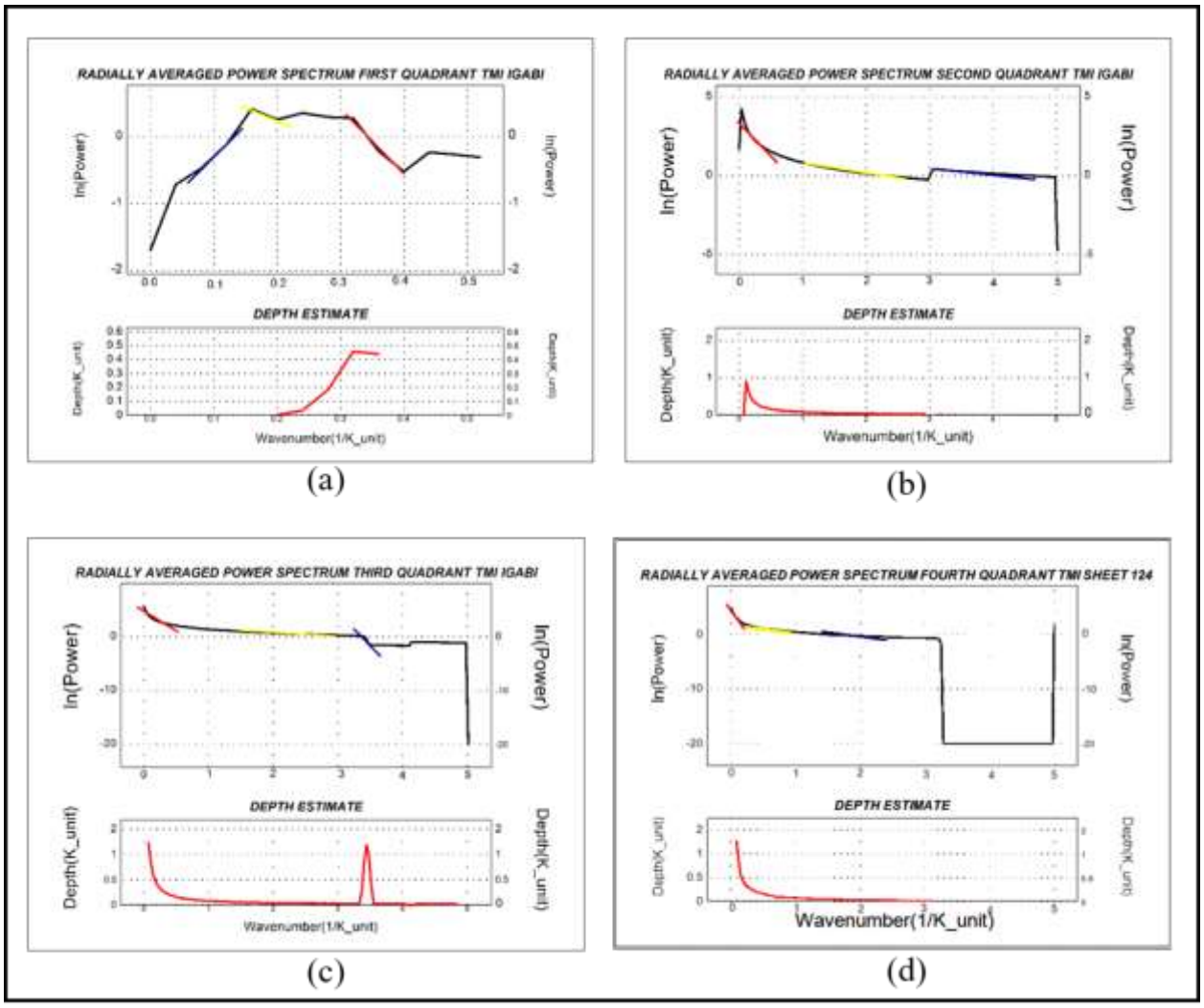

Figure 8: RAPS on TMI first quadrant (a), second quadrant (b), third quadrant (c), and fourth quadrant (d).

4.6 Euler Deconvolution

The use of Euler deconvolution as an interpretation tool to determine source location of magnetic field's anomalies. Thompson (1982) developed the technique and applied it to profile data, and Reid et al. (1990) developed the more widely used version for grid-based data. Euler deconvolution method is used to estimate the locations and depths for several linear subsurface features such as (lineaments, geological contacts, faults, dikes, sills). The 2-D Euler deconvolution is used not only to delineate major subsurface structures but also to determine the structural indices of them (Sultan *et al.,* 2017). For mineral exploration, the depth estimates are used to define the location and depth of source that cause a magnetic anomaly (Whitehead, 2010). The Euler Deconvolution was applied to the Total Magnetic Intensity Map at Structural index 0.0, 1.0and 3.0 respectively to obtain better solution shown in figure 10 with an average error in depth estimation less than the required maximum 15% tolerance and window size, and the result with the least unreal solutions was adopted. The linear forms with the same depths generally correspond to faults. Each structural index represents different models (Table 2). The SI for any given anomaly may be determined indirectly by seeking the SI value that yields least local perturbation of the calculated background value (Barbosa *et al.*, 1999). The application of extended Euler deconvolution creates a large volume of information.

The magnetic map (Fig. 10a) show Euler deconvolution map at Structural index 1.0. It is modeled as sills and dykes. It displays prisms with large circles intertwined with straight lines; observed as dyke and sills short colour range. The result show colours coded circles, the circles colors indicate depth range and the size defines depth variation for the magnetic map ranges from less than <189.6 m to over 852 m. The lineament trends are seen found in cluster lines trending in NW-SE direction on the windowed result. It also shows the depths are deeper compare to the other rock types present on the map. The area of very low magnetic intensities is seen not to have any point circles indicating their various depths.

The magnetic map (Fig. 10b) show Euler deconvolution map at Structural index 3.0. It is modeled as sphere. It shows the windowed result occurring as spheres bodies of circles in cluster form with a common axis connecting them. Euler deconvolution magnetic map at structural index 3.0 (Fig. 10b) depth ranges from less than 386.5 m to greater than 2054 m. The solution produces realistic results which were consistent with the type of geologic model in the study area.

Table 2: Structural Index Values. (Reid *et al.,* 2013)

Model	**Magnetic SI**
Point, sphere	3
Line, cylinder, thin bed fault	2
Thin sheet edge, thin sill, thin dyke	1
Contact of infinite depth extent	0

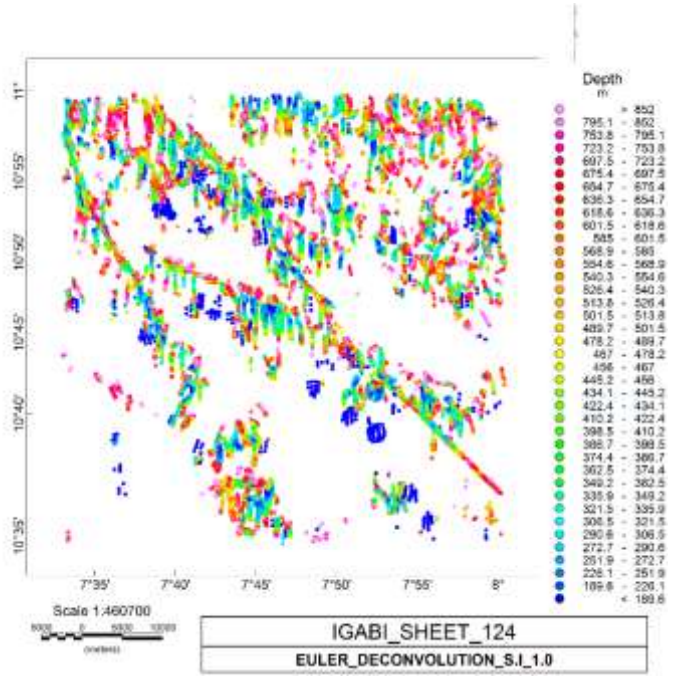

(a)

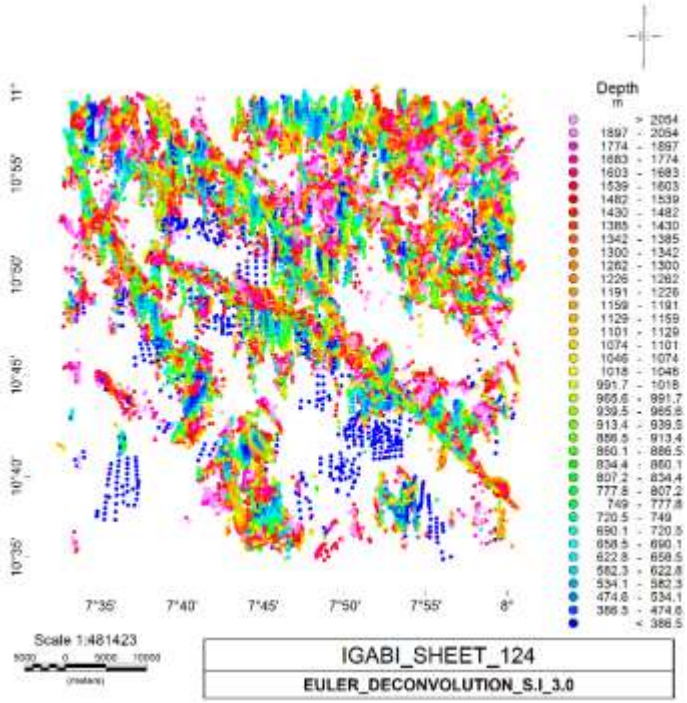

(b)

Figure 10: (a) Euler Deconvolution of the Magnetic Map at Structural Index 1.0 (b) Euler Deconvolution for Magnetic Map at Structural Index 3.0

5.0 Conclusion

This research has effectively revealed the depths to the magnetic basement with the aid of Total gradient amplitude, Tilt horizontal derivative, Spectral Depth Analysis and Euler deconvolution methods using aeromagnetic data of Igabi area North western part of Nigeria. The Total gradient amplitude was applied on the total magnetic field intensity of the data; it shows the edges locations of the magnetic sources in vertical dimensions. The positions and trends of these anomalies are similar to those of the total horizontal derivative map with the depth of over 2 *km*. Total gradient amplitude and Source Parameter Index techniques were used to calculate the depth to the magnetic basement sources. They reflected similar results for estimating the basement depths ranging from -63051.21*m* to -7639.14 *m*. Furthermore, the tilt angle derivative maps results revealed the various anomalous trends and to source depth of magnetic value over 3000 *m.* Spectral Analysis suggests depth to magnetic sources range from deep, intermediate and shallow with depths between 40 and 60*km* for shallow and 600 *m* to *1200 m* for intermediate and 900 *m* to 3200*m*for deep sources on the magnetic map. The obtained Euler anomalies depths range from <386.5 m to >2054 m for the magnetic map. This study, therefore, suggest rocks that varies in depth based on their lithologies that led to variations in the measured magnetic field parameters in the study area.

6.0 Conflicts of Interest:

The authors declare that there is no competing interest in this research

7.0 Acknowledgement:

The authors are grateful to Nigerian Geological Survey Agency (NGSA) for the release of aeromagnetic dataset of Igabi for academic research. Many thanks to the anonymous reviewers for their painstaking efforts in bringing out the best in this manuscript.

References

Ansari, A. H., and Alamdar, K. 2009. Reduction to the Pole of Magnetic Anomalies Using Analytic Signal. *World Applied Sciences Journal, vol.* 7, *no*. 4, pp. 405-409.

Bhattacharyya, B., K., 1966, Continuous spectrum of the total magnetic field anomaly due to a rectangular prismatic body: *Geophysics*, vol. 31, pp. 99-121

Barbosa,V., Silva, J. and Medeiros W. 1997. Gravity inversion of basement relief using approximate equality constraints on depths: *Geophysics*, vol. 62, pp. 1745-1757.

Barbosa, V. Sliva, J. Medeiros, v. 1999. Stability analysis and improvement of structural index in Euler deconvolution.*Geophysics,* vol. 64 no.1, pp. 48-60

Barbosa,V., Silva, J. and Medeiros W. 1999a. Gravity inversion of a discontinuous relief stabilized by weighted smoothness constraints on depth: *Geophysics*,vol. 64, pp. 1429-1437.

Barbosa,V., J. Silva, and W. Medeiros, 1999b, Stable inversion of gravity anomalies of sedimentary basins with nonsmooth basement reliefs and arbitrary density contrast variations: *Geophysics*, vol. 64, pp. 754-764.

Blanco-Montenegro, I., Torta, J.M., García, A. and Araña, V. 2003. Analysis and modelling of the aeromagnetic anomalies of Gran Canaria (Canary Islands): *Earth Planet. Sci. Lett.,* vol. 206, pp. 601–616.

Cooper, G. R. J. and Cowan, D. R. 2006. "Enhancing potential field data using filters based on the local phase," *Computers & Geosciences*, vol. 32, no. 10, pp. 1585–1591.

Cooper, G. R. J. 2013. "Reply to a discussion about the 'Hyperbolic tilt angle method' by Zhou et al," *Computers & Geosciences*, vol. 52, pp. 496–497.

Cordell, L., and Grauch V.J.S. 1985. Mapping basement magnetization zones from aeromagnetic data in the San Juan basin, New Mexico, In: Hinzc W.J. (Ed.). The utility of regional gravity and magnetic anomaly maps, *Soc. Expl. Geophys*., pp. 181–197.

Ferreira, F. J. F., de Souza, J., Bongiolo, A. D. B. E. S. and de CastroL. G. 2013. "Enhancement of the total horizontal gradient of magnetic anomalies using the tilt angle," *Geophysics*, vol. 78, no. 3, pp. pp. 33–41.

FitzGerald, D., Reid, A. and McInerney P. 2003. New discrimination techniques for Euler deconvolution: 8th SAGA Biennial Technical Meeting and Exhibition, pp. 7-10.

Gallardo-Delgado, L., Perez-Flores, M., and Gomez-Trevino E. 2003. A versatile algorithm for joint 3D inversion of gravity and magnetic data: *Geophysics*, vol. 68, pp. 949-959.

Ghosh, G. K., Gupta, R. D., Khanna, A. K., and Singh S. N. 2012. Application of Euler Deconvolution of Gravity and Magnetic Data for Basement Depth Estimation in Mizoram Area. *Geohorizons*, pp. 13-19. http://dx.doi.org/10.3997/2214-4609.20143715.

Hansen, R.O., Pawlowski, R.S., and Wang X. 1987. Joint use of analytic signal and amplitude of horizontal gradient maxima for three dimensional gravity data interpretation, 57th annual international management, *Soc. Expl. Geophys*.pp. 100–102.

Hinze, W.J., Ralph, R.B.V., and Saad A.H. 2013. Gravity and Magnetic Exploration (Cambridge. England, Camb. Univ. Press), 512 p.

Hubbard, F.H. 1975. Precambrian crustal development in western Nigeria: indications from the Iwo region. *Gcol. Soc. Amer Bull*. vol. 20, no. 1, pp.117-139.

Jeng, Y., Lee, Y. L., Chen, C. Y., and Lin M. J. 2003. Integrated signal enhancements in magnetic investigation in archaeology. *Journal of Applied Geophysics, vol. 53*, pp. 31–48. http://dx.doi.org/10.1016/S0926-9851.

Kivior, I., and Boyd, D. 1998. Interpretation of the Aeromagnetic Experimental Survey in the Eromanga/Cooper Basin: Can. *J. Explor. Geophys*, vol. 34, no. 1-2, pp. 58-66.

Li, X., 2003. On the use of different methods for estimating magnetic depth: *The Leading Edge*, pp. 1090-1099.

Martins, C., Barbosa, V. and Silva J. 2010. Simultaneous 3D depth-to-basement and density contrast estimates using gravity data and depth control at few points: *Geophysics*, vol. 75, pp. pp. 21-28.

Martins, C., Lima, W.,BarbosaV. and Silva J. 2011a. Total variation regularization for depth-to-basement estimate: Part1—Mathematical details and applications: *Geophysics*, vol. 76, pp. 11-12.

Martins, C., Lima, W., Barbosa, V. and Silva J. 2011b. Total variation regularization for depth to-basement estimate: Part2—Physicogeologic meaning and comparisons with previous inversion methods: *Geophysics*, vol.76, pp. 13-20.

McCurry, P. 1975. The geology of the Precambrian to Lower Palaeozoic Rocks of Northern Nigeria. In: *Geology of Nigeria*, edited by C.A. Kogbe. pp. 25-45.

Mishra, D.C. and Naidu P.S. 1974. Two dimensional power spectral analysis of aeromagnetic fields. *Geophys Prosp.* vol. 22, pp. 345-534.

Milligan, P. R., Reed, G., Meixner, T. and Fitzgerald D. 2004. Towards automated mapping of depth to magnetic/gravity basement — examples using new extensions to an old method. *ASEG 17th Geophysical Conference and Exhibition, Sydney.* vol. 373, pp. 129-139.

Nabighian, M.N. 1972. The analytic signal of two-dimensional magnetic bodies with the polygonal cross-section: its properties and use for automated anomaly interpretation, *Geophysics*, vol. 3, no. 37, pp. 507–517.

Nabighian, M.N. and Hansen R.O. 2001. Unification of Euler and Werner deconvolution in three dimensions via the generalised Hilbert transform: *Geophysics*, vol. 66, pp. 1805-1810.

NGSA, 2010. Modified Geological map of Nigeria, extracted and digitized from sheet 1:100,000. Nigerian Geological Survey Agency, Abuja, Nigeria

Obaje N. G. 2009. Geology and Mineral Resources of Nigeria, Lecture Notes in Earth Sciences. Springer Dordrecht Heidelberg, London New York. 221p.

Ogezi, A.E.O. 1988. Origin and Evolution of the Basement Complex of North-western Nigeria in the light of new Geochemical and Geochronological Data: In: Precambrian Geology of Nigeria, Geological Survey of Nigeria (Ed). pp. 301–312.

Okpoli, C.C., and Akingboye, A.S. (2019). Application of High-resolution gravity data for litho-structural and depth characterisation around Igabi, Northwestern Nigeria, NRIAG Journal of Astronomy and Geophysics 8(1): 231-241

Okpoli, C.C., and Akingboye, A.S. (2020). Application of Airborne Gravimetry Data for Litho-Structural and Depth Characterisation of Precambrian Basement Rock (Northwestern Nigeria) *Geophysica* 55(1–2), 3–21

Okpoli, C.C**.** and Eyitoyo, F.B. (2016). Aeromagnetic Study of Okitipupa Region, Southwestern, Nigeria. *International Basic and Applied Research Journal*, 2(7): 1-20.

Okpoli, C.C, Ogbole, J.O., Oyeshomo, A.V., Okanlawon, G.O. (2022). Mineral exploration of Iwo-Apomu Southwestern Nigeria using aeromagnetic and remote sensing *The Egyptian Journal of Remote Sensing and Space Sciences* 25, 371–385

Oyawoye, A.O. 1964. "The Geology of Nigerian basement complex. *Journal of Nigeria Min. Geol.* vol. 1, no. 2, pp. 87-193.

Rahaman, M. A. and Ocan, O. O. 1987. Relationship in the Precambrian migmatitic gneisses of Nigeria. *Journal of Mining and Geology.* vol. 15, no. 1, pp. 23-32.\

M. Rajaram, 2009. What's new in interpretation of magnetic data?, *Geohorizons.* pp. 50–51

Reid, A. B., Allsop, J.M., Granser, H., Millet, A. J. and Somerton, I.W. 1990. Magnetic interpretation in three dimensions using Euler Deconvolution: *Geophysics*, vol. 55, pp. 80–91.

Reid, A.B., Jorg E., and Susan J. Webb. 2013. Avoidable Euler Errors – the use and abuse of Euler deconvolution applied to potential fields. *Geophysical Prospecting*, pp. 1–7.

Roest, W. R., Verhoef, J., and Pilkington M. 1992. Magnetic interpretation using the 3-D analytic Signal. *Geophysics, vol. 57, no.* 6, pp. 116-125. http://dx.doi.org/10.1190/1.1443174

Saad, S.A., 2017. High Resolution Gravity, Helicopter Magnetic, and Electromagnetic Study, Haile Gold Mine, South Carolina. Bachelor of Science King Saud University. 61p.

Salem, S. Williams, J. D. Fairhead, D. Ravat, and Smith, R. 2007. "Tilt-depth method: a simple depth estimation method using first-order magnetic derivatives," *The Leading Edge*, vol. 26, no. 12, pp. 1502–1505.

Salem, A., Williams, S., Fairhead, D., Smith, R. and Ravat D. 2008. Interpretation of magnetic data using tilt-angle derivatives. *Geophysics*, vol. 73, pp. 1–10.

Silva, J., Costa, D. and Barbosa V. 2006. Gravity inversion of basement relief and estimation of

density contrast variation with depth: *Geophysics,* vol. 71, pp. 51-58.

Silva, J., Oliveira, F. Barbosa, V. and Campos H.V. 2007. Apparent-density mapping using entropic regularization: *Geophysics,* vol. 72, pp. 51-60.

Silva, J., Oliveira, A. and Barbosa V. 2010a. Gravity inversion of 2D basement relief using entropic regularization: *Geophysics.* vol. 75, pp. 29-35.

Silva, J., Vasconcelos, S. and Barbosa V. 2010b. Apparent-magnetization mapping using entropic regularization: *Geophysics.* vol. 75, pp. 39-50.

Spector, A., and Grant F.S. 1970. Statistical Models for interpreting aeromagnetic data. *Geophysics,*vol. 35, pp. 293-302.

Sultan, S.A., Mohamed E., Abou, H.M., Mahmoud, E.I., Ahmed K., Enas, M. and Abd E. 2017. Implementation of magnetic and gravity methods to delineate the subsurface structural features of the basement complex in central Sinai area, Egypt. *NRIAG Journal of Astronomy and Geophysics.* pp. 1-28. https://doi.org/10.1016/j.nrjag.2017.12.002.

Tatiana, F.Q. and Angelo, S. 1998. Exploration of a lignite bearing in Northern Ireland, using Maurizio ground magnetic.*Geophysics,* vol. 62, no. 4, pp. 1143-1150.

Thompson, D. T. 1982. EULDPH: A new technique for making computer assisted depth estimates from magnetic data*: Geophysics*, vol. 47, pp. 31–37.

Thurston, J. B., and Smith R. S. 1997. Automatic conversion of magnetic data to depth, dip, and susceptibility contrast using the SPITM method. *Geophysics.*vol. 62, pp. 807- 813.

Tsepav, M.T. 2018. Comparative Analysis of the Source Parameter Imaging and Spectral Depth Techniques of Determining Depth to Magnetic Sources in a Sedimentary Environment, using Aeromagnetic Data. *International Journal of Scientific & Engineering Research.* vol. 9, no. 3, pp. 1535- 1543.

Verduzco, J. D. Fairhead, C. M. Green, and MacKenzie C. 2004. "New insights into magnetic derivatives for structural mapping," *The Leading Edge,* vol. 23, no. 2, pp. 116–119.

Whitehead, N., 2010, montaj Grav/Mag Interpretation, tutorial and user guide, Geosoft Incorporated